PHOTOGRAPH THIS SHEET

DTIC FILE COPY

AD-A215 927

DTIC ACCESSION NUMBER

LEVEL

INVENTORY 1

R/D 5949-PH-02

DOCUMENT IDENTIFICATION

DASH45-88-M-0168

2 JULY 1988

DISTRIBUTION STATEMENT A

Approved for public release;
Distribution Unlimited

DISTRIBUTION STATEMENT

ACCESSION FOR		
NTIS	GRA&I	X
DTIC	TAB	☐
UNANNOUNCED		☐
JUSTIFICATION	per form 50	
BY		
DISTRIBUTION /		
AVAILABILITY CODES		
DIST	AVAIL AND/OR SPECIAL	
A-1		

DISTRIBUTION STAMP

DTIC
ELECTE
DEC13 1989
S D
E

DATE ACCESSIONED

DATE RETURNED

89 12 12 013

DATE RECEIVED IN DTIC

REGISTERED OR CERTIFIED NO.

PHOTOGRAPH THIS SHEET AND RETURN TO DTIC-FDAC

DTIC FORM 70A
MAR 86

DOCUMENT PROCESSING SHEET

PREVIOUS EDITION MAY BE USED UNTIL STOCK IS EXHAUSTED.

[redacted]

DISCLAIMER NOTICE

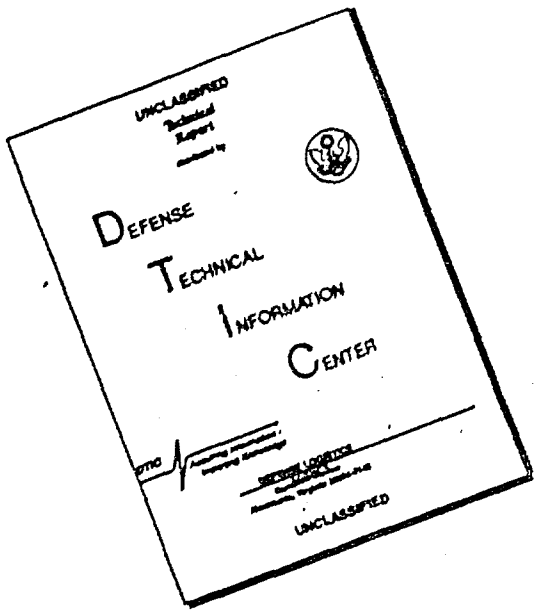

THIS DOCUMENT IS BEST QUALITY AVAILABLE. THE COPY FURNISHED TO DTIC CONTAINED A SIGNIFICANT NUMBER OF PAGES WHICH DO NOT REPRODUCE LEGIBLY.

SAGAMORE IX

CONFERENCE ON CHARGE, SPIN AND MOMENTUM DENSITIES

Luso – Bussaco, PORTUGAL

26 June – 2 July 1988

ABSTRACTS

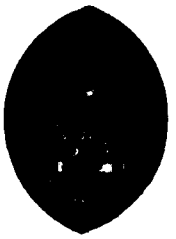

DEPARTAMENTO DE FISICA

UNIVERSIDADE DE COIMBRA- PORTUGAL

INDEX

P1 - Spin densities

and theoretical

X-Ray Diffraction, Electron Densities and Chemical Bonding

W.H.E.Schwarz, L.Mensching, K.Ruedenberg and L.Miller
(Theoretical Chemistry Groups, University of Siegen, Germany, and Iowa State University, Ames, USA)

Molecular electron densities are often examined in the form of difference densities (DDs). Conventionally they are defined with respect to the superimposed densities of the spherically averaged atoms. These DDs are denoted here as Total Difference Densities (TDDs). They are particularly useful for the discussion of the electrostatic fields created by molecules in the space around them. However, only atoms with spatially nondegenerate ground states are of necessity spherically symmetric. Most atoms with open p and d shells are not, and consequently their TDDs are often dominated by quadrupolar density distributions which are the result of the orientation of the undeformed atomic groundstates. These orientational effects can be quite large and hide the genuine atomic deformations that are associated with molecule formation. Because of the superposition of the atomic orientation and chemical deformation effects, it is intrinsically difficult to compare TDDs of different systems, and the term "deformation densities" for them seems unfortunate.

As a more appropriate quantity for the elucidation of the nature of chemical binding, the Chemical Deformation Density (CDD) is defined here with respect to the reference density of a promolecule whose unperturbed atoms, in addition to being positioned at their correct places in the molecule, also have their multipoles appropriately oriented. This procedure is also a natural one from an information theoretical point of view. The approach is applied to theoretical densities to a series of small molecules and to experimental x-ray scattering data of a series of organic molecular crystals.

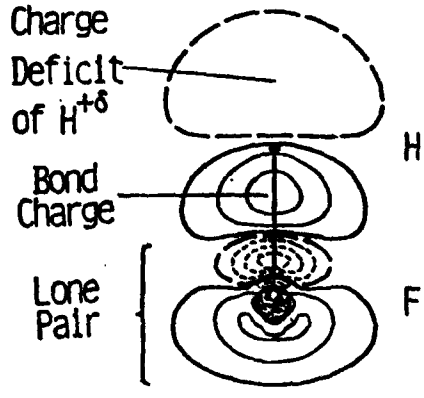

The eigenvalues of the orientation tensors are compared with theoretical Mulliken populations. The CDDs offer a coherent picture of bond and lone pair density deformations. In particular fluorine, oxygen and nitogen compounds do no longer exhibit exceptional features.

The effects of hybridization, charge transfer and constructive interference on the electron deformation density maps of the first-row hydrides

Arthur A. Low and Michael B. Hall

Abstract

Standard deformation density maps, molecular density minus the sum of the spherical atom densities, may show some features contrary to what is expected by chemical intuition. This is due to the effects of hybridization and charge transfer on these maps which can mask the effects of constructive interference of atomic orbitals. Changing the choice of promolecule to the sum of valence-state hybrid atoms partitions the effects of hybridization out of the standard deformation density maps. Another choice of promolecule, namely the sum of the densities of the singly occupied GVB pair orbitals, subtracted from the total GVB molecular density, produces deformation density maps which partitions out the effects of charge transfer. This produces deformation density maps which only show the effects of constructive interference. These deformation density maps and various difference density maps of the first-row hydrides, AH_x (A = Li-F, x=1-4) are computed in order to observe the effects of hybridization, charge transfer and constructive interference on their deformation density maps.

Polarisation effects in Mg(water)6(hydrogenmaleate)2

P. Vanhouteghem, A.T.H. Lenstra and H.J. Geise
U.I. Antwerpen, Dept. Chemistry,
Universiteitsplein 1,2610 Wilrijk (Belgium)

An electron density study of the title compound was carried out using low temperature (100K) X-ray and neutron data. A nearly symmeric deformation density was observed in the hydrogen maleate moiety, even though the moiety has no crystallographically imposed symmetry. This observation points towards a large internal consistency in the data. With the Mg-ion at an inversion center, the metal coordination contains three independent water molecules. Only one shows a deformation density compatible to the distortion expected from an 'ab-initio'model (fig.1.). The distortion observed in the H2O bisecting plane of the two other water molecules has no parallel in the theoretical model (fig.2.), and is believed to be connected to the electrostatic potential created by the H2O neighbours. Hence, we calculated a defotmation potential from the difference between the multipole and an independent atom model, leaving out the water molecule under investigation. For the 'normal' H2O we find a nearly constant deformation potential (fig.3.), whereas the maps for the 'anomalous' H2O entities show much larger variations(fig.4.). The observed polarisation follows an electronic redistribution along an equipotential plane.

figure 1.

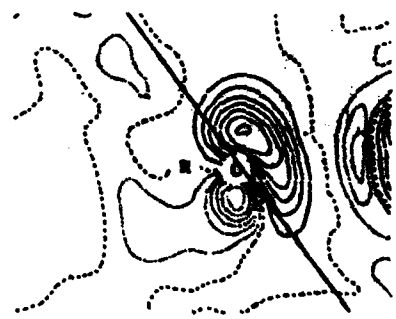

figure 2.

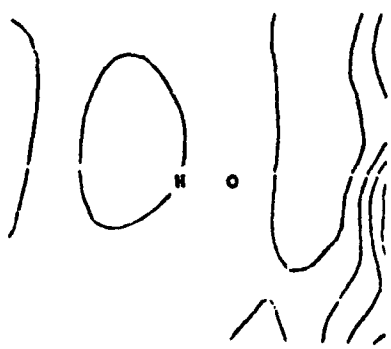

figure 3.

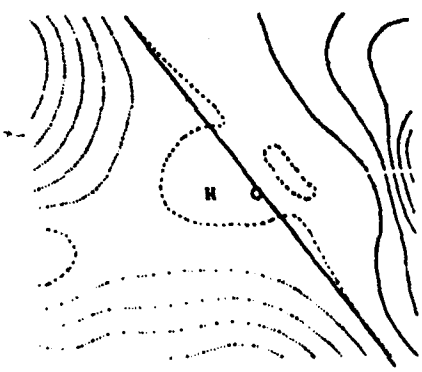

figure 4.

Transferability of localized charge distributions

Harry Bruning and Dirk Feil

Chemical Physics Laboratory , Twente University
PB 217, 7500AE Enschede, the Netherlands.

The calculation of the electrostatic interaction in molecular complexes requires knowledge of the charge distribution in the monomers. Only for small molecules this knowledge can be obtained by quantumchemical calculation. The present study shows how the electron density distribution in crown ether molecules can be obtained by addition of fragment densities, derived from Hartree-Fock-Slater calculations on H_2O, CH_3OH, CH_3OCH_3. The constructed density is compared with the electron density distribution in 18-crown-6. Transferability is seen to apply to polarisation by ionic guests as well.

Electron Density in the Alkali Halide Crystals *

G.Böbel, P.Cortona a. F.G.Fumi
Dipartimento di Fisica, Università di Genova and CISM/MPI - GNSM/CNR, Unità di Genova (Italy)

Structure factors at room temperature are computed for LiF, NaF, NaCl and KCl by means of theoretical ionic form factors and theoretical Debye-Waller factors. The values obtained are compared with the best available experimental data. For LiF and KCl - for which good experimental data are available - we find excellent agreement, while for NaCl and NaF the discrepancies that we find can be rather naturally attributed to deficiencies of the experimental data. We conclude that there is no apparent need to question the validity of the DW theory as recently proposed in the literature.

---

*Supported in part by a grant from the Italian Research Council under the French-Italian Scientific Collaboration Agreement.

Electronic density study of hexacarbonyl -μ -di-t-butylacetylene -di-iron : a joint experimental and theoretical study.

by F.Baert and A.Laamyen UFR de physique Bat. P5
USTL 59655 Villeneuve d'Ascq France.
R.Wiest and M.Benard lab. de chimie quantique Institut Le Bel
Université L. Pasteur F67000 Strasbourg France.

An experimental electronic density and a theoretical analysis of the title compound have been undertaken.

The deformation density calculated with $X\text{-}X_{HO}$ formalism at a resolution of 0.90 $Å^{-1}$ ($I>1\sigma(I)$) shows four peaks around the Fe atoms. Multipole refinements with different models have been done using the Stewart modified by Hansen & Coppens formalism. The best results are obtained with the $4s^2$ incorporated the core and the $3d^6$ represented by the monopole 1. There is good agreement between the model dynamic maps and the experimental ones. The d orbital occupancies have been calculated from the multipole parameters.

Interpretation of the experimental and theoretical results shows that the formal double metal-metal bond postulated for $Fe_2(CO)_6(HC_2H)$ does not involve any direct coupling between the metal d electrons. The metal-metal interactions are effective through back-donation processes involving either the semi-bridging carbonyl or the acetylenic group.

These results are compared to those of the $Co_2(CO)_6$ $((CH_3)_2C_2$ compound which has two more electrons.

E.N. Maslen & N. Spadaccini
Crystallography Centre, University of WA, Nedlands 6009 West Australia

Medium Range Atomic Overlap in Perovskite Structures

$\Delta\rho$ maps for the transition metal KMF_3 perovskites have been studied extensively (Kijima et al, 1981; 1983; Miyata et al, 1983; Spadaccini, 1988). The divalent metal M is octahedrally coordinated to F atoms, with eight second nearest neighbour K atoms located on the <111> vectors. $\Delta\rho$ along the M-F bonds is increasingly depleted from the Mn to the Ni structure, as expected for an exchange term. The density along the M-K vectors is correspondingly enhanced. The $\Delta\rho$ map for $KMnF_3$ is shown in Fig. 1.

There is a structural cavity midway between and 2Å from the K atoms, which is 2Å and 2.8Å from the F and M atoms respectively. $\Delta\rho$ at that location is .6eÅ^{-3} for $KMnF_3$, progressively decreasing to a hollow of -.8eÅ^{-3} in the Ni structure. This cannot result from random error and is unlikely to arise from related systematic errors in four separate experiments. Though too far from the atomic sites to be attributed to known chemical effects, the changes through the series are highly correlated with other significant features. $\Delta\rho$ values at the F atom, in the metal e_g orbital and the density in the metal t_{2g} orbital projected onto the MF_4 plane, are plotted against cell dimension for the series in Fig. 2. The variation with cell size is linear. This is not surprising for $\Delta\rho$ near the atomic sites, since the overlap between the metal atom and the F ligands must vary in a regular manner. However $\Delta\rho$ at the structural cavity shows the same linear variation. Because the feature is far from the nuclei, at a site of low electrostatic potential, this has significant implications for the related series high T_c $LnBa_2Cu_3O_7$ superconductors.

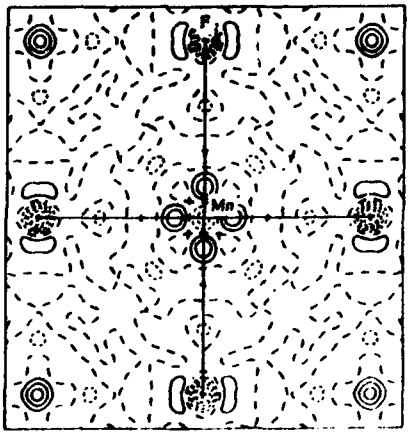

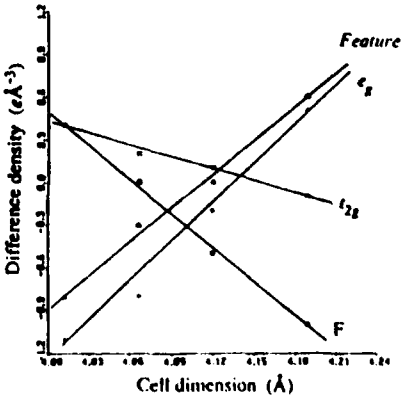

QUANTUM TOPOLOGY APPROACH TO THE X-RAY DIFFRACTION RESULTS INTERPRETATION: ETHANE, ETHYLENE, ACETYLENE

KAPPHAHN M., TSIREL'SON V.G., OZEROV R.P.

Mendeleev Institute of Chemical Technology
Moscow 125820, Miusskaya Sq. 9, U.S.S.R

The chemical bond in molecules and crystals is often analysed in terms of the deformation density distribution. There exists another approach, suggested by Bader et al., which is dealing with topological analysis of the electron density distribution $\rho(r)$. This method is based on the René Thom catastrophe theory, concerned with different types of critical points revealing and consists of the $\rho(r)$ function and its derivatives estimation at that points. The advantage of this approach is the absence of a reference model induced into calculations.

The method of topological analysis of the $\rho(r)$ function derived from X-ray diffraction measurements is presented, structure analysis drawbacks (such as finite resolution, series termination effect etc.) being taken into account. Topological results for the experimental density $\rho_{exp}(r)$ of the crystals C_2H_6, C_2H_4, C_2H_2 are compared with those from the free molecular theoretical density $\rho_{th}(r)$ of C_2H_6, C_2H_4 and C_2H_2. An estimation of the influence of atomic thermal motions on the topological characteristics of $\rho(r)$ for the single, double and triple bonds has been given. The topological method allows to receive more information from the X-ray diffraction experiment, for instance, about intermolecular interactions, chemical reactivity and the most probable sides of electrophilic and nucleophilic atacks.

CHARGE DENSITY DISTRIBUTION, ELECTROSTATIC POTENTIAL AND COMPLEX FORMATION ABILITY OF SOME NEUTRAL AGENT

VARNEK A.A., GLEBOV A.S., KUZNETSOV A.N.

Mendeleev Institute of Chemical Technology,
Miusskaja Sq. 9, Moscow 125820, U.S.S.R.

Charge density and electrostatic potential (MEP) distributions have been obtained from the quantum-chemical calculations (MNDO, CNDO/2) and crystal chemistry considerations for some macrocyclic and phosphorganic agent.

1. Introduction of the electron acceptors (Cl, NO_2) into the benzene rings of dibenzo-18-crown-6[2] (I) reduces the ligand donor atoms charges. Elecdonor alkilic substitutors (Me+Oct) practically do not influence on the charge distribution in the macrocycle cavity. The negative MEP values in the macrocycle cavity in dichloro-(II) and dinitro-(III) derivatives I are lower than in I but in dialkile derivatives (IV) MEP distribution is same as in I. The stability of the complexes II-IV with metal cations reduction, regarding unsubstituted ligand, which has been observed experimentally, can be explained by some reasons: by cation-ligand interaction energy lowering in II and III, by solvatation effects in IV. These suppositions have been confirmed by molecular mechanics and Monte-Carlo methods.

2. The complex formation and extraction ability in the rows $(MeO)_3PO$-$(MeO)_2MePO$-$MeOMe_2PO$-Me_3PO and $(MeO)_2(OH)PO$-$(MeO)Me(OH)PO$-$Me_2(OH)PO$ increases while changing the alkoxylic radical by alkilic one. As the result of such substitution, according calculations the donor oxygen atom (O_{ph}) negative charge is reduced while the MEP value in O_{ph} vicinity becomes more negative. So that MEP distribution describes the complex formation ability better than atomic charge analysis.

THE ATOMIC AND ELECTRON STRUCTURE REFINEMENT WITH THE USE OF A PRIORY CHEMICAL BOND DATA

KRASHENINNIKOV, M.V.

Mendeleev Institute of Chemical Technology,
Moscow 125820, Miusskaja Sq. 9, U.S.S.R.

The free spherical symmetric atom model is usually used in the traditional methods of covalent crystal structure refinements. Some of the important atomic electron density distribution peculiarities are not taken into account in this model. This can influence the thermal parameters, scale factor and other values refined as well as the experimental electron density distribution. Many models (aspherical form factors, double atom, κ-technique, multipole decomposition) had been suggested in order to improve the situation.

The iteration refinement procedure is proposed which is dealing with the standard parameters determination as well as full crystal potential distribution in reciprocal space calculation. The corrections to the experimental and calculated structure factors can also be determined in the linear quantum perturbation theory approach the Fermi wave number being taken into account. Procedure converges to the self consisted parameters into the limit accepted.

MOESSBAUER-EFFECT STUDY OF THE SPIN-DENSITY-WAVES IN Cr+

S. M. Dubiel, Institute of Metallurgy. Academy of Mining and Metallurgy. PL-30-059 Krakow, Poland

A fascinating phenomenon known as spin-density waves (SDW) in metallic chromium was up-to-now mainly investigated by means of neutron and x-ray scattering techniques. We will show that also a spectroscopy based on the Moessbauer effect i.e. a technique involving the hyperfine interactions can successfully be applied to study SDW and associated effects.

In particular, using ^{119}Sn-site Moessbauer effect we succeeded (i) to observe the so-called spin-flip transition in metallic chromium i.e. the transition at T≈123K between transversally and longitudinally polarized SDW and (ii) to detect the third harmonic of SDW and to quantitatively determine its relative contribution.

In our model study we show that the ^{119}Sn-site Moessbauer spectra are well sensitive to such parameters characterizing SDW like: higher order harmonics, their signs and their relative amplitudes. This can be taken as a challange for the Moessbauer spectroscopy in its future applications in this field.

+ Supported in part by The Institute of Physics. PAN, Warsaw

18 P1.12

THE INFLUENCE OF INEQUIVALENT COBALT SITES ON THE SPIN AND ORBITAL MAGNETIC MOMENTS IN YCo_5

Barbara Szpunar and Vedene H. Smith, Jr.
Department of Chemistry, Queen's University
Kingston, Ontario, Canada K7L 3N6

Self-consistent band structure calculations for YCo_5 have been performed with the linear-muffin-tin-orbital, atomic-sphere approximation (LMTO-ASA) method. In contrast to earlier calculations, the 2c and 3g cobalt sites were not constrained to be equivalent. The resulting differences in the local electronic and magnetic structure of these cobalt sites are discussed.

Sagamore IX Conference on Charge, Spin and Momentum Densities, 26 June-2 July 1988.

ANTIFERROMAGNETISM IN SEMICONDUCTORS RELATED TO HIGH TRANSITION TEMPERATURE SUPERCONDUCTING COPPER OXIDES

Barbara Szpunar and Vedene H. Smith, Jr.
Departments of Chemistry and Metallurgy
Kingston, Ontario K7L 3N6 Canada

The possibility of obtaining itinerant antiferromagnetic ordering in the new high T_c superconductors is explored by means of self-consistent spin polarized calculations for the non-superconductor $YBa_2Cu_3O_6$, which is related to the superconductor $YBa_2Cu_3O_{7-\delta}$ and for models of doped copper oxide planes. Investigation of both the ferromagnetic and antiferromagnetic ground states reveals the former to be unstable and the latter to be stable. Our calculations show that for antiferromagnetic ordering of copper magnetic moments in the Cu2-O plane, there is a Peirels-type gap around the Fermi energy and $YBa_2Cu_3O_6$ in particular, is semiconducting as observed experimentally. Comparison is made with recent neutron diffraction studies.

Sagamore IX Conference on Charge, Spin and Momentum Densities, 26 June-2 July 1988.

MAGNETISATION DENSITY DISTRIBUTION IN AN ORGANO-BIMETALLIC COMPLEX OF Cu(II), Ni(II)

B. Gillon*, Y. Journaux**, O. Kahn**

*Laboratoire Léon Brillouin (CEA-CNRS), CEN-Saclay
91191 Gif-sur-Yvette cedex, France
**Laboratoire de Spectrochimie des Eléments de Transition,
ERA 672, Université Paris-Sud, 91405 Orsay cedex, France

Organo-bimetallic complexes of 3d transition metals present a large variety of intramolecular magnetic interactions, at long distance, between the 3d ions, depending on the number and the nature of the ligands surrounding each metal. The determination of the magnetisation density is such systems, using the Polarised Neutron Diffraction method, yields direct information about the magnetic coupling and the role of the atoms of the organic bridge relating the metals ions.

In the complex Cu(Salen) $Ni(hfa)_2$, two oxygen atoms form the central bridge between the Cu^{2+} and Ni^{2+} ions :

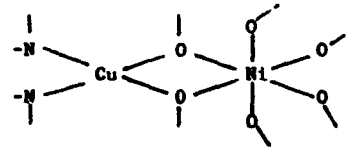

The experimental study was performed on the polarised neutron diffractometer 5C1 at the LLB in Saclay (France). Two sets of data have been collected using a lifting counter, for two different orientations ($\vec{a}$ vertical, then $\vec{b}$ vertical) of the same single crystal, at 2K under an applied field of 5 teslas. The whole set of 362 reflections permited to determine the three-dimensional image of the magnetisation density, using a multipole refinement method. A strong positive density on the Nickel and a weak negative density on the Cupper are observed, in agreement with a fundamental doublet spin state. The spin delocalisation on the ligands is discussed.

Spin and orbital effects in 5f compounds

G.H. Lander and M. Wulff

Commission of the European Communities, Joint Research Centre
European Institute for Transuranium Elements
Postfach 2340, D-7500 Karlsruhe
Federal Republic of Germany

Abstract

The 5f electrons that surround the nucleus of the light actinide elements (U, Np, Pu, and Am) behave in a different way to the 4f electrons that one finds in the lanthanide series. The large spatial extent of these 5f electrons means that they interact strongly with electrons belonging to neighboring atoms. In this sense, of course, they are not unlike 3d electrons. However, their f quantum number means that they have a strong orbital character. What happens to this orbital character when there is a strong hybridization between the 5f electrons and neighboring d or p electrons? This is an important question in actinide physics. It has been addressed by theory and in this paper we shall discuss neutron experiments that address this issue.

In the light actinides with less than a half-filled shell the orbital (L) and spin (S) moments are opposite if we follow Hund's rule and Russell-Saunders coupling. The magnetization densities of the L and S components have a different spatial density. Thus, we can imagine a cancellation of L and S when integrated over all space, but for a certain Q (scattering vector) a finite moment exists. We will discuss the unusual magnetic form factors of PuSb, $PuFe_2$, and UFe_2 that demonstrate this point.

COEXISTENCE OF MAGNETIC AND NON MAGNETIC CERIUM IN Ce_2Sn_5 OR Ce_3Sn_7

J.X. BOUCHERLE°, F. GIVORD*, P. LEJAY§, J. SCHWEIZER°, A. STUNAULT°

° Centre d'Etudes Nucléaires, DRF/SPh-MDN, 85 X, 38041 Grenoble Cedex, France.
* Centre National de la Recherche Scientifique, Laboratoire Louis Néel, 166 X, 38042 Grenoble Cedex, France.
§ Centre National de la Recherche Scientifique, CRTBT, 166 X, 38042 Grenoble Cedex, France

Polarised neutron experiments have been performed on Ce_2Sn_5 and Ce_3Sn_7 single crystals. These two compounds are orthorhombic superstructures of the cubic intermediate valence compound $CeSn_3$. In both compounds the Ce atoms occupy two sites : Ce_I is similar to the Ce site in $CeSn_3$, with 12 Sn neighbouring atoms, and Ce_{II} has 2 Ce and 10 Sn neighbouring atoms. Both compounds are very anisotropic : their magnetisations are the largest when the field is applied parallel to $\vec{a}$.
The magnetisation density maps evidence that only the Ce_{II} atoms are magnetic and particularly that no magnetisation is present around the Ce_I atoms.
The form factors of the Ce_{II} atoms are different in the two compounds. In Ce_2Sn_5 it corresponds to a spherical Ce^{3+} whereas in Ce_3Sn_7 it is much steeper, which corresponds to a more delocalised magnetisation in the (b, c) plane.

P2 - Charge densities

ELECTRON DENSITY OF SACCHARINE DERIVATIVES

J. Buschmann, R. Rudert, P. Luger (Institut für Kristallographie, Free University of Berlin), G. Trummlitz (Dr. K. Thomae GmbH, Biberach)

To get behind the mystery why artificial sweeteners have specific tastes we are doing structure and electron density investigations on sweet and bitter tasting saccharine derivatives. The results are compared with previous, more general and theoretical work in this field.

Shallenberger and Acree (1967)[1] found that many sweet tasting compounds have two electronegative atoms with a distance of 2.5 to 4 Å between them with one of them having a covalently bonded hydrogen atom, and Kier (1972)[2] added as another characteristic a hydrophobic molecular part away from the two electronegative atoms. Trummlitz (1985)[3] carried out quantum chemical calculations with CNDO/2 for saccharine derivatives and obtained as one result that the keto oxygen atom of the sweet tasting compounds carries a negative charge.

X-ray and neutron single crystal diffraction experiments were performed on sweet and bitter tasting saccharine derivatives at the temperature of 123 K. The difference Fourier synthesis for the sweet tasting compound shows the keto oxygen atom (se Fig. 1, atom O3) with additional negative charge. Further work on a bitter tasting derivative is in progress.

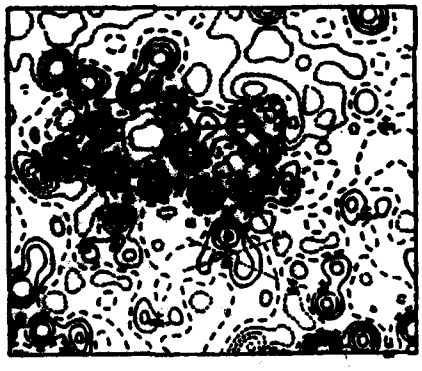

Fig. 1 : X-N difference Fourier synthesis of UHAF 50 Na, cut through molecular plane, contour interval 0.1 e/Å^3

References:
1. Shallenberger, R.S., Acree, T.E., "Molecular Theory of Sweet Taste", Nature, 216, 480 (1967).
2. Kier, L.B. "A Molecular Theory of Sweet taste", J. Pharm. Sci., 61, 1394 (1972).
3. Trummlitz, G. (1985) unpublished results.

Acknowledgement: The authors gratefully acknowledge the scientific and experimental help of Dr. David Gregson at the SILOE reactor of C.E.N.G at Grenoble. This work has been funded by the German Federal Minister for Research and Technology (BMFT) under the contract number 03-LUIFUB-0-01-55 and the Fonds der Chemischen Industrie.

Charge Density Studies of Tetramethylthiuram Disulfide and Tetraethylthiuram Disulfide

Yu Wang and J.H. Liao; Department of Chemistry, National Taiwan University, Taipei, Taiwan, R.O.C.

Two Thiouram disulfide compounds were studied by X-ray diffraction at 105K, 143K. The room temperature structures were studied previously (Wang; Liao; Ueng; 1986). Tetramethylthiuram disulfide, monoclinic, C2/c ; T=143K, a=9.524(4), b=9.911(3), c=11.795(1)Å, β=99.22°(1), Z=4, $\lambda(MoK_\alpha)$=.71069 Å. Final R=.031 for 2881 reflections. Tetraethylthiuram disulfide, monoclinic, $P2_1/c$, T=105K, a=10.922(3), b=15.946(4), c=8.444(1) Å, β=91.92(1)°, $\lambda(MoK_\alpha)$=.71069 Å. Final R=.029 for 5772 reflections. They both contain a disulfide bridge connecting two identical thiuram parts. The sulfur-sulfur bonds with length 2.0052(4), 2.0057(4) Å respectively, are essentially single bonds. The tetramethyl derivative undergoes a phase transition at ~140K, the high temperature molecular structure has a C_2 symmetry. There are C=S double bond and C-S single bond in both molecules. The accumulation of electron density along the C-N and C-S bonds in the experimental deformation density maps are as expected. The lone pair feature around sulfur atom is also observed. The peculiar appearance along sulfur sulfur bond are comparable with other recent works containing sulfur sulfur bond. Some theoretical model density calculations could be adopted to give reasonable explanation.

Wang, Yu;Liao, J.H. and Ueng, C.H.

Acta Cryst.(1986)C42,1420-1423

N-O bonding electron in p-nitrobenzene derivatives

by Shigeru Ohba and Yoshihiko Saito, Keio University, Japan

In the X-X and X-N maps of p-nitropyridine N-oxide(3) at 30 K, the N-O bonding electron was not significantly observed. [1] However, the bonding peak was detected in $LiNO_3.H_2O$ at 120 K. [2] An ab initio MO calculation using MIDI4 * basis set (double-zeta + polarization function) suggests that the deformation density is almost the same for HNO_3 and NO_3^-. [2] The unknown factor is (3) is the interactions between the nitro group and the aromatic ring. In the present work, the deformation densities of p-dinitrobenzene(1) and p-nitrobenzoic acid(2) has been determined at 120 K. (1) $P2_1/a$, Z=2, $2\theta_{max}$(Mo Kα) =110°, R=0.055 for 2045 unique reflections. (2) A2/a, Z=8, $2\theta_{max}$= 120°, R=0.042 for 3930 reflections. X-X maps on the benzene rings are shown in Fig. 1. The deformation densities on the nitro planes are also given, because the dihedral angles between the nitro group and the benzene ring are (1)10.2° and (2)14.8°. The N-O bonding peak as well as the lone-pair peaks of the terminal oxygen atoms are clearly observed. Neutron work is now in progress.

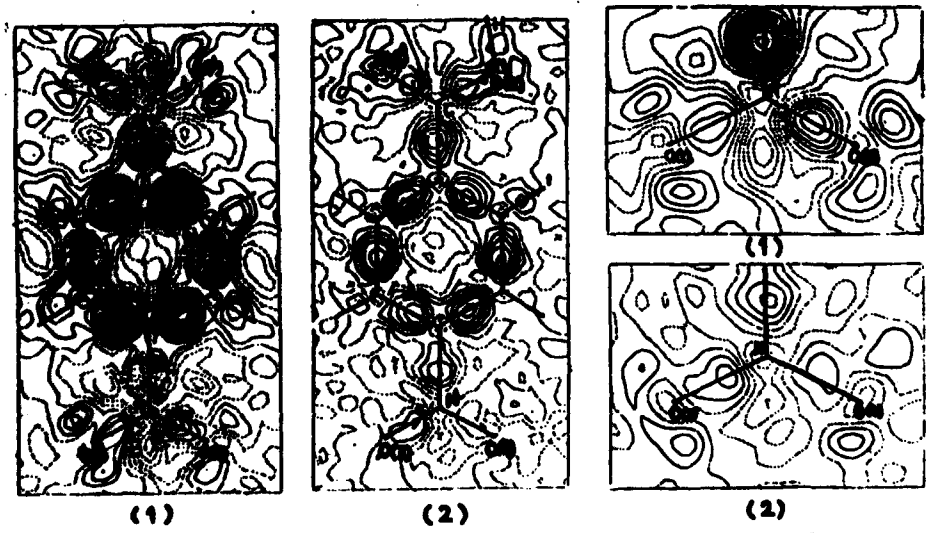

Fig. 1. Deformation density. Contour interval 0.1 eÅ^{-3}. $\sigma(\Delta\rho)$=0.05 eÅ^{-3}.

(1)Coppens & Lehmann(1976)Acta Cryst.B32.1777 (2)Ohba,Kikkawa & Saito(1985) Acta Cryst. C41,10 (3)Kikkawa,Ohba,Saito,Kameta & Iwata(1987) Acta Cryst. B43, 83.

L. BRAMMER and E.D. STEVENS

Department of Chemistry, University of New Orleans, New Orleans Louisiana 70148, U.S.A.

THE EXPERIMENTAL ELECTRON DENSITY DISTRIBUTION OF BIS(TRIPHENYLPHOSPHINE)DICHLORONICKEL(II), $NiCl_2(PPh_3)_2$

The experimental electron density distribution of bis(triphenylphosphine) dichloronickel(II) has been determined from single crystal X-ray diffraction data, collected at 94(1)K. The molecule crystallizes in space group P2/c (No.13), with Z=2, requiring two-fold molecular symmetry about the central nickel atom. A total of 25248 intensities were measured (excluding standard reflections), to a resolution of $\sin\theta/\lambda = 1.0\text{Å}^{-1}$. Symmetry averaging yielded 13288 independent reflections, R(int) = 0.019, after correction for absorption. Coventional refinement using constrained hydrogen positions yielded R = 0.038, GOOF = 1.274 for 8610 reflections with $F>3\sigma(F)$.

The tetrahedral rather than square-planar coordination of the ligands in $NiCl_2(PPh_3)_2$ is unusual for a d^8 Ni complex. This requires a paramagnetic electronic structure and leads to a substantial dipole moment, a property which is yet to be investigated using the X-ray measurements. The total electron density has been modelled using atom-centered multipole density functions. Deformation density maps show accumulation of electon density between all covalently bonded atom pairs. In addition, phosphorus lone-pair peaks consistent with the principally σ-donor bonding mode of phoshine ligands are observed.

The support of the Science and Engineering Research Council (UK) in the form of a NATO postdoctoral fellowship to L.B. is acknowledged.

ELECTRON DENSITY IN PEPTIDE DERIVATIVES (N) ACETYL-TRYPTOPHANE-METHYLAMIDE (Ac tr) AND (N) ACETYL-DEHYDROPHENYLALANINE-METHYLAMIDE (Ac Δ)

M. SOUHASSOU, C. LECOMTE and A. AUBRY
Laboratoire de Minéralogie-Cristallographie, UA CNRS N°809, Université de Nancy I, BP 239, 54506 Vandoeuvre les Nancy Cédex, France

Ac tr, group space $P2_12_12_1$, Mo(Kα), 100°K, $\sin\theta/\lambda$ max = 1.14 Å^{-1}, 10527 collected data, 2800 unique, multipole analysis, Rw = 2.7 %, GOF = 0.86.

Ac Δ, group space C_2, Mo(Kα), 100°K, $\sin\theta/\lambda$ max = 1.36 Å^{-1}, 14666 reflections collected, in which 6135 unique, multipole analysis, Rw = 2.23, GOF = 1.00 ($\sin\theta/\lambda$ < 0.9 Å^{-1}, Rw = 1.31%, GOF = 0.87).

Déformation maps calculated from $|F_{obs}|$ and multipole phases, fig. 1 and 2 are view of Ac tr and Ac Δ respectively, deformation maps of Ac tr (fig. 3) and of Ac Δ (fig. 4) , will be commented and compared.

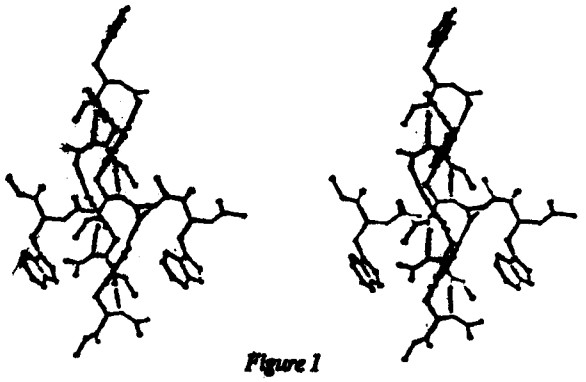

Figure 1

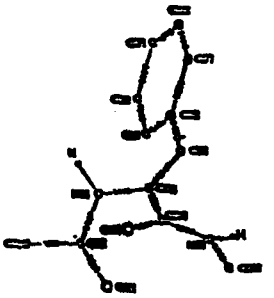

Figure 2

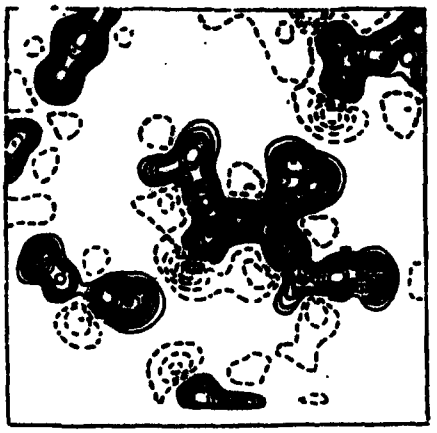

Figure 3

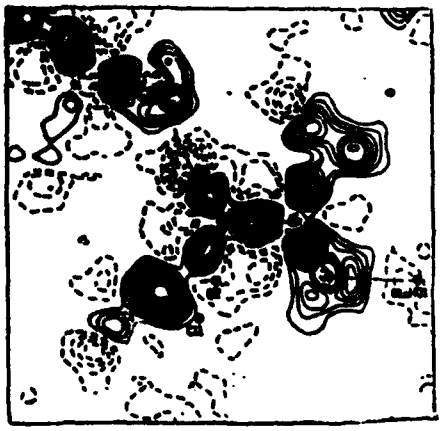

Figure 4

TRYING TO GET INFORMATION ABOUT THE Pd-Pd BOND

Jean-Paul MANGEOT, Claude LECOMTE, Yves DUSAUSOY
Laboratory of Crystallography, UA CNRS N°809, University of Nancy I, B.P. 239, 54506 Vandoeuvre Cédex, France

$Pd_2Cr_2Cp_2(\mu_3CO)_2(\mu_2CO)_4(PEt_3)_2$ (figure 1). Centrosymmetric ($P2_1/c$, a = 10.706, b = 9.375, c = 17.370 Å, β = 115.38°, Z = 2). 24181 reflections were measured at 100 ± 5 K with MoKα radiation using graphite monochromator (CAD4 - ω/2θ scan, 7 standard reflections, $\sin\theta/\lambda \leq 1.35$ Å^{-1}). After treatment absorption, corrections and averaging, the number of independant reflections were 9138 with $I > 4\,\sigma(I)$ and 4020 having $\sin\theta/\lambda > 0.80$ Å^{-1}. After an H.O. anharmonic Gram-Charlier refinement and a multipolar analysis, (R = 0.023 ; Rw = 0.024) deformation and dynamic model map (figures 2 and 3) were calculated and will be commented and compared to the only theoretical data available (Pd-Pd) (figure 4).

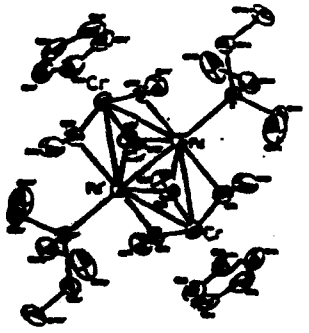

Figure 1
Ortep diagram of the molecule

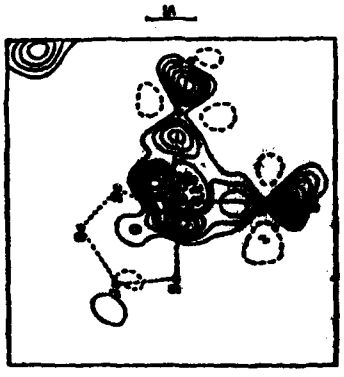

Figure 2
Dynamic model density map of the C_3 Cr C_1 plane
$\rho_{max} = 0.7$ e/Å^3

Figure 3
Déformation density map of the Pd-Pd C_2 plane
$\rho_{max} = 2.3$ e/Å^3

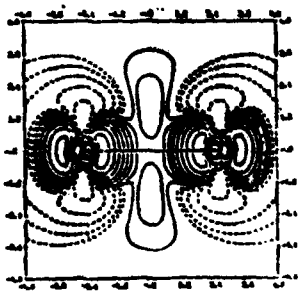

Figure 4
Deformation density map of the Pd_2 molecule ($\rho_{max} = 0.6$ e/Å^3)
(Shim and Gingerich, J. Chem. Phys., 1984, 80 (10) 5107)

11K Charge density study of a short non-bonded S...O contact in 2,5-diaza-1,6dioxa-6a-Thiapentalene

by

P. Becker (1), B. Fabius(2), C. Cohen-Addad (3), F.K. Larsen (2), M.S. Lehmann (4)

(1) Lab. Cristallographie, CNRS, BP 166, 38042 Grenoble, France. (2) Dept. Chemistry, Aarhus Univ., DK-8000 Aarhus C, Denmark. (3) Lab. Spectrométrie Physique, Univ. Grenoble, BP 87, 38402 St Martin d'Hères, France. (4) Institut Laue-Langevin, BP 156, 38042 Grenoble, France.

Many compounds containing the X-S---O configuration (X = O, C) exhibit very short S--O distances. In order to understand the molecular stabilization in these compounds, we have undertaken an investigation of the charge density by X-ray diffraction measurements at 11K in 2,5-diaza-1,6-dioxa-6a-thiapentalene (S---O distance of 1.84 Å).

The charge density distribution in the molecule was not clearly understood from previous 122 K X-ray and neutron measurements [1] [2]. In the present study, results obtained with 11K X-ray diffraction measurements and aspherical atom refinement using the program MOLLY [3] are presented.

The static deformation model maps are in good agreement with the theoretical maps obtained from a previous local-density-functional calculation. The electric dipole moment calculated from multipole parameters, σ (11K) = 2.0D is in good agreement with the value known from a microwave study, σ = 2.88 (2) D [4].

The mechanism proposed to interpret the X-S...O interaction depends on the electronegativity of X and involves a σ -type coupling between oxygen and sulfur p and a stabilization of the molecule through sulfur d orbitals. The experimental charge distribution obtained at 11K supports this theory and leads to the rejection of the previous controversial deduction that oxygen is in a special state with little hybridation. A reinvestigation of the previous 122K X-ray data using also the MOLLY program is qualitatively consistent with the results.

[1] Becker, P., Cohen-Addad, C., Delley, B., Hirshfeld, F.L. & Lehmann, M.S., Applied Quantum Chemistry, 361, Reidel Publishing Company (1986). [2] Cohen-Addad, C., Lehmann, M.S., Becker, P. & Davy, H., Acta Cryst., in press. [3] Hansen, N.K & Coppens, P., Acta Cryst., A34, 909 (1978). [4] Larsen, N.W., Nygaard, T., Pedersen, C.Th., Davy, H., J. Mol. Struct., 118, 89 (1984).

ELECTRON DENSITY DISTRIBUTION IN TERBIUM TRIS (TRIFLUOROMETHANESULPHONATE) NONAHYDRATECRYSTALS

By - A. Chatterjee*

Crystallography Centre, The University of Western Australia, Nedlands, Australia 6009

The electron density distribution in crystalline title compound has been investigated with the single crystal X-ray diffraction method. Evidence for trigonally deformed distribution of 4f electrons around terbium atom was observed in the final difference Fourier synthesis. The residual electron densities were observed to be dependent on the orientation of the water oxygen atoms. The salient features of the contour maps have been discussed.

* Present address: - Department of Physics, Univ. Rajshahi, Rajshahi 6205, Bangladesh.

ELECTRON DENSITY DISTRIBUTION IN SPINEL-LIKE $CdCr_2Se_4$

TSIREL'SON, V.G., BOROVSKAJA, T.N., OZEROV, R.P.

Mendeleev Institute of Chemical Technology Miusskaja Sq. 9,
Moscow 125820, U.S.S.R.

BUTMAN, L.A.

Institute of General and Inorganic Chemistry Leninsky P. 31,
Moscow 117071, U.S.S.R.

Semiconducter and ferrimagnetic spinel-like $CdCr_2Se_4$ has been investigated by X-ray diffraction precision experiment (Sintex $P2_1$ diffractometer, Mo-$K\alpha$ radiation, spherical sample diameter 0,13mm, 4487 reflections in two Ewald sphere octants, $\sin\theta/\lambda \leq 1{,}054 Å^{-1}$). Cprrections for absorption, anomalous scattering, TDS and Bacher-Coppens extinction have been applied. High angle refinements converged to R=0,013, R_w=0,0135, S=1,053.

The deformation electron density distribution has been calculated in the usual way. The peculiarities have been analysed in terms of electron orbitals population. For example, the preferred occupation of e_g and a_{1g} orbitals has been found in Cr^{3+} ion in trigonal distorted octahedron leading to uncoupled electron spins in this ion. There are no covalent peaks on the Se-Cr bond line. But the peak $0{,}2 eÅ^{-3}$ has been found 1,1Å away from the Cr^{3+} ion near the octahedron face. This has been attributed to the preferred occupation of $d_{xy,xz}$ and d_{yz} orbitals with the group π ligand orbital.

CHARGE DENSITY STUDIES IN TWO HEXAGONAL LAVES PHASES

M.J.M. de Almeida, M.M.R. Costa, J.A. Paixão

Centro FC1, INIC - Departamento de Física, Universidade de Coimbra
3000 Coimbra, PORTUGAL

Accurate measurements of X-ray intensities were made at room temperature on two single crystals A and B of $TiMn_2$ ($0.06 \times 0.06 \times 0.10$ mm^3 and $0.07 \times 0.08 \times 0.08$ mm^3, respectively) and one single crystal of $TiFe_2$ ($0.08 \times 0.06 \times 0.05$ mm^3). Both structures are hexagonal Laves phases (space group $P6_3/mmc$).

Reflection intensities inside an Ewald sphere of radius $1.25 Å^{-1}$ were accurately measured with a CAD4 diffractometer, Mo-Kα radiation and a graphite monochromator in ω-2θ scans.

The usual geometrical corrections and an empirical absorption correction were applied to the data.

High-angle refinements ($\sin\theta/\lambda \geq 0.6 Å^{-1}$) of positional and thermal parameters and a scale factor were carried out from each data set. Anomalous dispersion corrections were included in the spherical atomic scattering factors. Extinction was empirically corrected through a g parameter refined will all data.

Difference density maps (with corresponding error maps) were compared and discussed in terms of a subsequent least-squares refinement of 3d orbital populations.

ELECTRON DENSITY OF A CUBIC LAVES PHASE, $TiCo_2$

Ana Matos Beja, L. Alte da Veiga, L.C.R. Andrade, M.M.R. Costa, J.A.Paixão

Centro FCl,INIC - Departamento de Física da Universidade de Coimbra
3000 Coimbra, PORTUGAL

The Laves phase $TiCo_2$ has a cubic structure of type $MgCu_2$, space group Fd3m (8 empirical formulas per unit cell).

A single crystal of $TiCo_2$ (size:0.10 x 0.12 x 0.15 mm^3) has been studied by X-Ray diffraction technique, using a CAD4 diffractometer with a plane graphite monochromator and Mo-Kα radiations; the unit cell parameters are: a = b = c = 6.7048(9)Å, α = β = γ = 89.99(2)°, and all the atomic positions are fixed by symmetry.

The diffracted intensities of the whole sphere of reflection were measured in ω-2θ scans, up to $\sin\theta/\lambda = 1.19Å^{-1}$. The total number of independent reflections with $I \geq 3\sigma$ is 114.

The whole set of collected data (including weak reflections, total of 18528 reflections) was corrected for Lorentz and polarisation factors, and for the variation in the intensity of standard reflections; an analytical absorption correction was applied to these data.

The 114 independent "observed" reflections resulting from averaging the corrected intensities were used to carry out least squares refinements; the thermal parameters were obtained from high-angle refinements ($\sin\theta/\lambda \geq 0.65$), together with the scale factor.

An empirical extinction parameter, g, was refined after words (keeping all other parameters fixed) with all 114 independent reflections.

Difference density maps and the corresponding error maps were obtained and a subsequent refinement of the occupation parameters of 3d orbitals has been undertaken.

ELECTRON DENSITY OF FeF_2

M.J.M. de Almeida, M.M.R. Costa and J.A. Paixão

Centro FC1, INIC - Departamento de Física, Universidade de Coimbra
3000 Coimbra, PORTUGAL

The electron density distribution of FeF_2 (rutile type structure, a=b=4,7008Å, c=3,3100Å) has been derived at room temperature from accurate X-ray diffraction measurements (CAD4 diffractometer, Mo-K_α radiation, graphite monochromator, ω-2θ scans, all octants of Ewald sphere cut to $\sin\theta/\lambda = 1.1Å^{-1}$) carried out on two single crystals A and B (with approximate dimensions 0.10 x 0.11 x 0.12 mm^3 and 0.07 x 0.08 x 0.11 mm^3, respectively).

Corrections for Lorentz, polarisation and absorption were applied to 2897 reflections from crystal A and 3014 from crystal B, before averaging equivalent reflection intensities.

Atomic and temperature parameters and a scale factor were refined from high-angle data ($\sin\theta/\lambda \geq 0.6Å^{-1}$; 123 independent reflections from crystal A and 125 from crystal B), against a spherical model with atomic scattering factors corrected for anomalous dispersion. An extinction parameter, g, was refined using the whole data set.

Difference density maps and error maps were calculated. The significant features were interpreted in terms of 3d orbitals population.

ELECTRON DENSITY OF NiF_2

M.M.R. Costa, M.J.M. de Almeida, J.A. Paixão and L.C.R. Andrade

Centro FC1, INIC - Departamento de Física, Universidade de Coimbra
3000 Coimbra, PORTUGAL

Precision X-ray diffraction measurements were carried out at room temperature on a single crystal of NiF_2 (rutile type structure, a=b=4.6499Å; c=3.0833Å) with approximate dimensions $0.04x0.03x0.08mm^3$ (CAD4 diffractometer, Mo-Kα radiation, graphite monochromator, ω-2θ scans, all octants of an Ewald sphere with radius $1.1Å^{-1}$).

Lorentz polarization and analytical absorption corrections were applied to 2560 reflections.

Data processing was carried out in two different ways (DP1 and DP2):

DP1: Atomic and temperature parameters and a scale factor were refined from high-angle data (99 independent reflections with $\sin\theta/\lambda \geq 0.6Å^{-1}$) against a spherical model with atomic scattering factors (International Tables for X-Ray Crystallography) corrected for anomalous dispersion.

An empirical extinction correction was applied to the data based on an extinction parameter, g, refined with the whole data set.

Difference density maps and error maps were obtained; the results were interpreted in terms of refined occupation parameters of 3d orbitals.

DP2: A multipole refinement of all parameters including the symmetry allowed multipole populations was made using the program MOLLY and 1543 reflections with $I>3\sigma$ corrected for isotropic, type I, Gaussian extinction (Becker and Coppens).

DISTRIBUTIONOF THE ELECTRON DENSITY IN THE A15 PHASE Cr_3Si

Ana Matos Beja, L. Alte da Veiga and M.M.R. Costa
Centro FCl, INIC - Departamento de Física, Universidade de Coimbra
3000 Coimbra, PORTUGAL

One of the most interesting structural features of A15 phases is the existence of linear atomic chains in three orthogonal directions; the interatomic distances along these chains are shorter than those predicted by metallic radii criteria. Among the A15 phases (cubic, space group Pm3n), Cr_3Si is one of those in which the shortening of these distances is more important; the unit cell has 8 atoms with symmetry fixed positional parameters.

Accurate measurements of X-ray single crystal diffraction data were undertaken. Six data sets were obtained, using four distinct crystals of the same sample, and two different radiations (Ag-Kα and Mo-Kα), at room temperature and, for one of the crystals, also at low temperature (T ≈ 170K). For every crystal, data within an Ewald sphere (with radius 1.25$\AA^{-1}$) were collected with a CAD4 diffractometer, plane graphite monochromator, in ω-2θ scans. The measured cell parameters were in good agreement; reflections with $I \geq 3\sigma$ (about 4600) have been used to perform the analysis: usual geometrical corrections, the correction resulting from differences in intensities of standard reflections, and two different absorption corrections have been applied. After averaging, 145 independent reflections were used to perform least squares refinements; scale factor and thermal parameters were refined from high-order data ($\sin\theta/\lambda \geq 0.6$).

An empirical extinction parameter, g, has been refined with all data.

The results obtained from the different data sets are compared.

Careful measurement of absolute scale factor confirmed the value obtained from high-order refinements.

Difference density maps together with error maps were compared, and no significant covalency along the linear atomic chains was found.

P3 - Momentum densities

Electron Correlation Effect in the Momentum Distributions of Transition Metals

Shinya WAKOH and Makoto MATSUMOTO
University of Library and Information Science. Tsukuba 305. Japan

In the 1970's band-theoretical calculations of Compton profiles of vanadium and chromium were published (Wakoh S and Yamashita J 1973 J. Phys. Soc. Japan Vol. 35 1406. Rath J. Wang C S. Tawil R and Callaway J 1978 Phys. Rev. Vol. B8 5189. Wakoh S. Kubo Y and Yamashita J 1976 J. Phys. Soc. Japan Vol. 40 1049) and they were compared with the available experimental Compton profiles. Recent experimental multiple scattering profiles of vanadium (Rollason A J. Holt R S and Cooper M J 1983 Phil. Mag. B Vol. 47 51) and chromium (Cardwell D A 1987 thesis at Univ. of Warwick. Cooper M J. Cardwell D A and Wakoh S 1988 Phil. Mag. to be published) have been processed by the Monte Carlo method (Felsteiner J and Pattison P 1975 Nucl. Instrum. Meths. Vol. 124 449). and therefore their single scattering profiles are very much reliable. The differences between the experiments and the theories. which were estimated by the band-theoretical one-electron approximation. show a significant feature: around the origin of the momentum axis the value of the theoretical Compton profiles is greater than that of the experimental ones. and at the higher momentum region it is the opposite. The general feature has been ascribed to the electron-electron correlation effect which was not taken into account in the one-electron band scheme. The difference curves (experiment-theory) are shown by dotted curves in figure 1 for vanadium. Although the effective one-electron potentials (modified X_α-potentials) used by the APW band calculations include some correlation effects like the LSD approximation (Gunnarsson O and Lundqvist B I 1976 Phys. Rev. Vol. B13 4274). the APW band theoretical Compton profiles do not include any dynamical correlation effects.

A theoretical correlation profile is proposed as follows:

$$J^{corr}(q) = -\int_{E_1}^{E_f}(1-n(E))\times J(q,E)dE + \int_{E_f}^{\infty} n(E)\times J(q,E)dE. \qquad (1)$$

Here. $n(E)$ is a Migdal function and $J(q,E)$ is a partial Compton profile contributed from the states whose energy is between $E-\Delta E/2$ and $E+\Delta E/2$. The function for vanadium is as follows:

$$n(E) = \begin{cases} 0.05+0.091(E/E_f) & for\ \ E<E_f \\ 0.141\times(E_0-E)^3/(E_0-E_f)^3 & for\ \ E>E_f\ . \end{cases} \qquad (2)$$

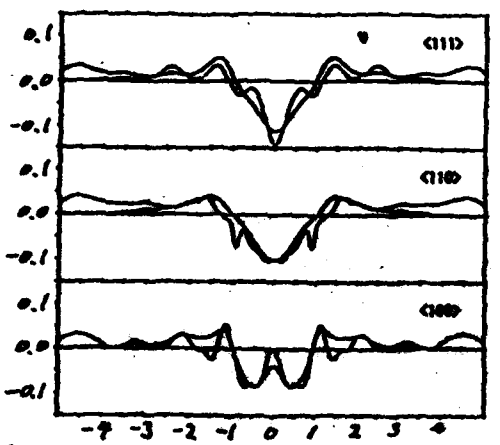

Figure 1.

Energies are referred to the bottom of the band (Γ_1). The theoretical correlation profiles obtained by equation (1) are shown by solid lines in figure 1.

It may be concluded that the correlation effects on the Compton profiles of vanadium and chromium whose Fermi levels are located at the middle of the d-bands, are predominantly due to the [illegible] function $n(E)$ for the d-bands.

Thanks are due to Dr M J Cooper and his Compton group at Univ of Warwick, and to SERC for financial support to visit the group.

HIGH RESOLUTION COMPTON PROFILE MEASUREMENTS USING 29.5 KeV SYNCHROTRON RADIATION

ITOH, F., SAKURAI, M. ,SUGAWA, T. and SUZUKI, K.
Institute for Materials Research, Tohoku Univ., Sendai 980, Japan
SHIOTANI, N., SAKAI, N. and MAO, O.
The institute of Physical and Chemical Research, Wakoh, Saitama 351-01, Japan
KAWATA, H., AMEMIYA, Y., and ANDO, M.
Photon Factory, KEK, Oho, Tsukuba 305, Japan

A high resolution Compton spectrometer using high energy X-rays from synchrotron radiation has been installed at Photon Factory of KEK. This spectrometer consists of 1) a curved crystal of Ge(220) to monochromatize incident photons into 29.5 KeV($\Delta E/E = 1.13\times10^{-4}$ at E=29.19 KeV), 2)a Cauchois-type curved crystal of Si(422)(the radius of bending is 2100 mm) for the energy analyzer of scatterd photons and 3) a position sensitive proportional counter or an Imaging Plate as the detector. The overall momentum resolution is 0.1 atomic units which is the highest resolution ever achieved for the energy of 29.5 KeV.

Compton profile measurements on single crystals of Al, Si, LiH, Li_2O, Li_3N and quasi-crystal of Li_6Al_4Cu have been successfully performed. The Compton profile of aluminum single crystal has shown a clear Fermi cutoff but at the same time some deviation from APW band theory is found to exist. The features of high resolution Compton profile measurement will be discussed particularly for Al single crystal in terms of J(q) and B(r).

The Compton-spectrometer at the HARWI-beamline (HASYLAB/DESY in Hamburg)

J.R.Schmitz, H.Schulte-Schrepping and W. Schülke
Institut für Physik, Universität Dortmund

The development of the Compton-spectrometer at the HARWI beamline is based on the following concept as sketched in Fig.1:

Monochromator: fixed exit double crystal monochromator (Si) with sagittal focusing. The first plane crystal is water-cooled, the second one is cylindrically bent and groove cut on the reflecting surface to suppress anticlastic bending.
In cooperation with the Hahn-Meitner-Institut (Berlin) the application of specially tempered Si-crystals is considered. These crystals would make possible further improvements in intensity by broadening of the single crystal reflection curves.

Analyzer: different setups are proposed:
1. energy-dispersive analysis by means of a Ge-SSD for Compton scattering with primary energies between 60 keV and 80 keV; momentum-resolution app. 0.8 atomic units.
2. crystal-dispersive analysis by means of a Cauchois-type analyzing crystal for primary energies from 30 keV to 40keV; momentum-resolution better than 0.1 atomic units, already tested at conventional X-ray sources.
For the present a Xe-filled position-sensitive proportional counter is used.
Enhanced efficiency and separation of higher harmonics will be obtained by a Ge-strip-detector with 200 strips, which is under development in cooperation with the Institut für Kernphysik , Kernforschungsanlage Jülich.
The Compton-spectrometer at the HARWI-beamline will be available as a user-experiment in 1989.

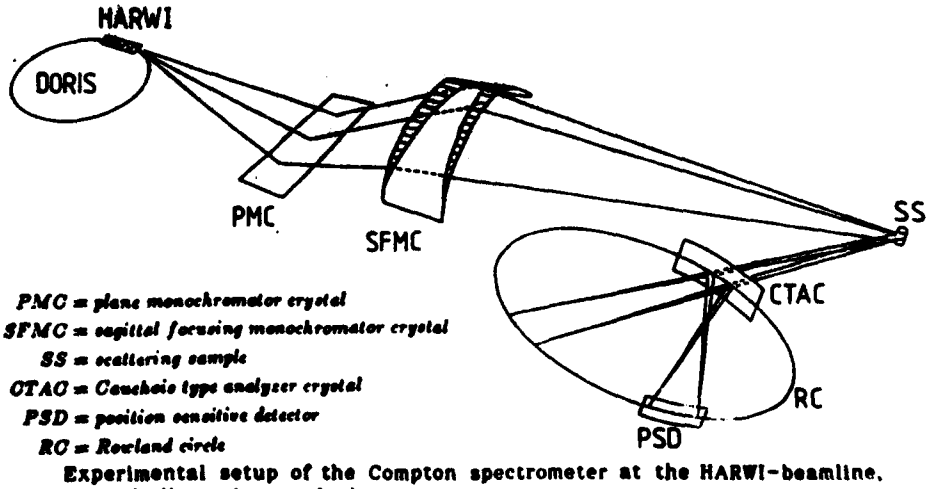

PMC = plane monochromator crystal
SFMC = sagittal focusing monochromator crystal
SS = scattering sample
CTAC = Cauchois type analyzer crystal
PSD = position sensitive detector
RC = Rowland circle

Experimental setup of the Compton spectrometer at the HARWI-beamline, crystal-dispersive analysis.

MAGNETIC X-RAY SCATTERING FACILITIES USING A HELICAL MULTIPOLE WIGGLER OF 6-GEV RING AT KEK

SAKAI, N., SHIOTANI, N., and ITO, M.
The Institute of Phys. and Chem. Research, Wako, Saitama 351-01, Japan.
ITOH, F., SAKURAI, M., and SUGAWA, T.
Institute for Materials Research, Tohoku Univ., Sendai 980, Japan.
KAWATA, H., AMEMIYA, Y., and ANDO, M.
Photon Factory, KEK, Oho, Tukuba 305, Japan.

Magnetic systems can be studied by using circularly polarized photons, because they interact with the electron spin and the electron orbital angular momentum through the relativistic electromagnetic interaction having an order of magnitude of E/mc^2, where E is a photon energy and mc^2 is the electron rest-mass energy. For the purpose of this magnetic experiment, a helical multipole wiggler is being installed [illegible] in a 6-GeV accumulation ring at KEK. [illegible] generate elliptically polarized [illegible] keV to 300 keV. One of the most important features of this insertion device is the high brilliance of 10^{15} photons/s · mm^2 · mrad^2 · 0.1%BW (6 GeV, 50 mA) having 50 % circular polarization for 80-keV X-rays. This will be used for the high resolution magnetic Compton profile measurement. The X-rays of lower energies with higher polarization will be used for the magnetic Bragg scattering. The ordinary high resolution Compton profile experiments can be also made by using 50-70 keV X-rays with brilliance of about 10^{16} photons/s · mm^2 · mrad^2 · 0.1%BW (6 GeV, 50mA). The practical designs of monochrometers, a Compton scattering spectrometer, and a magnetic Bragg scattering spectrometer will be presented.

46

P3.5

A. K. Singh, P. Genoud and T. Jarlborg

Département de physique de la matière condensée
Université de Genève
24, Quai Ernest Ansermet, CH-1211 Genève 4, Switzerland

Calculation of Compton profiles in ferromagnetic iron using LMTO wavefunctions

Abstract.
We report here the calculations of magnetic Compton profiles in ferromagnetic iron. A self-consistent together with a parametrized band structure calculations were performed using the linear muffin tin orbital method. Comparison with other calculations indicates that our results are in better agreement with the experimental values. Moreover the parametrized curve describes the measured magnetic Compton profiles in the low momentum region more precisely than any other calculation. These results confirm the analysis of positron annihilation data made by Genoud et al (*1988) which requires a parametrized band structure calculation. The main differences between both band structure concern the point N of the Brillouin zone: the large N-centered hole pocket of minority 3rd band given by the self-consistent calculation almost vanishes in the parametrized calculation. This trend is also supported by de Haas van Alphen measurements.

*) To be published in Journal of Physics F.

FORM FACTORS AND COMPTON PROFILES OF SOME METALS FROM AN ATOM-IN-JELLIUM-VACANCY MODEL

S.J. Mali, R.M. Singru and R.R. Mishra

Department of Physics, Indian Institute of Technology, Kanpur, 208016, India

and

D.G. Kanhere

Department of Physics, University of Poona, Pune, 411007, India

Some important properties about the charge and momentum densities have been calculated for metallic Be, Mg, Al, Si, Ge, Ca and Ag using local density approximation with the spherical atom-in-jellium-vacancy model. The starting point of each calculation was the computation of density function $\rho(\underline{r})$ using the atom-in-jellium-vacancy model [1]. Atomic form factors $f(\underline{G})$ were calculated for different metals and the results were found to agree well with experimental results. Transformation from the charge density $\rho(\underline{r})$ to the momentum density $\gamma(\underline{p})$ was carried out using the procedure of Burkhardt [2], Konya [3] and Coulson and March [4]. The results for $\gamma(\underline{p})$ were used to calculate the Compton profiles $J(q)$ and the momentum expectation values $\langle p^{-1} \rangle$, $\langle p \rangle$ and $\langle p^2 \rangle$ for various metals. These theoretical results were compared with experiment and satisfactory agreement was observed. In the case of metallic Al, the effect of various exchange correlation potentials on the form factors and on the $\langle p^{-1} \rangle$, $\langle p \rangle$ and $\langle p^2 \rangle$ values was examined.

[1] M. Manninen, P. Jena, R.M. Nieminen and J.K. Lee, Phys. Rev. B24, 7057 (1981); M.J. Puska, R.M. Nieminen and M. Manninen, Phys. Rev. B24, 3037 (1981).

[2] G. Burkhardt, Ann. Phys. (Leipzig) 26, 367 (1936).

[3] A. Konya, Hung. Acta Phys. 1, 12 (1949).

[4] C.A. Coulson and N.H. March, Proc. Phys. Soc. (London), A63, 367 (1950).

THE ELECTRON MOMENTUM DENSITY OF GALLIUM ARSENIDE

by
D.N.Timms and M.J.Cooper
Department of Physics, University of Warwick, Coventry. CV4 7AL.
R.S.Holt
Neutron Division, Rutherford Appleton Laboratory, Didcot, Oxon. OX11 0QX

The [100],[110],[111],[112] and [221] directional Compton profiles of gallium arsenide have been deduced from Compton scattering measurements on single crystal slices at gamma ray source energies of 412keV and 60keV. Both experimental systems detect profile anisotropies which are approximately 1% of the peak height $J(0)$. These profiles and their Fourier Transforms have been compared with the predictions of a pseudopotential band structure calculation. As expected the scale of the anisotropy is smaller than for germanium and is correctly predicted by the calculation. However, the calculation consistently underestimates the high momentum component of the charge density in all three directions.

THE DIRECTIONAL MAGNETIC COMPTON PROFILES OF IRON

by

S.P. Collins, D.N. Timms, M.J. Cooper, A. Brahmia and P.P. Kane.
Department of Physics, University of Warwick, Coventry. CV4 7AL.
R.S. Holt, Neutron Division, Rutherford Appleton Laboratory, Chilton Oxon. OX11 0QX.
D. Laundy, Daresbury Laboratory, Daresbury, Warrington, WA4 4AD.

Circularly polarised synchrotron radiation (CPSR) extracted from the SRS at Daresbury Laboratory has been used to determine for the first time, the directional magnetic electron momentum distribution in ferromagnetic iron. The data provide a much more critical test of band theory than is possible with polycrystalline samples. The scattering measurements were carried out in transmission geometry using a Ge (220) monochromator tuned to provide an incident energy of 56.8 keV, the scattered radiation being detected by an intrinsic germanium detector. A large single crystal wafer of silicon stabilised iron was aligned with the magnetic field parallel to one of the crystallographic directions ([100],[110],[111]) and the scattering vector. The directional magnetic Compton profiles determined from the unpaired spin distributions were compared with APW and KKR calculations for pure iron convoluted with the experimental resolution of 0.73a.u. The predicted directional differences are qualitatively confirmed by the new data although some interesting differences remain.

P3.9

X-Ray Inelastic Scattering Intensities Measured By Energy-Dispersive Diffractometry

Takao Iijima and Keiko Nishikawa
Department of Chemistry, Gakushuin University
Toshima-ku, Tokyo 171, Japan

In the energy-dispersive method, the theoretical expression of the inelastic scattering intensities to be compared with the experimental values are usually given by the approximation of neglecting the width of the Compton spectrum. The validity of this approximation has been numerically examined for the case of X-ray scattering from neon. The contribution from the tail of the Compton spectrum due to the inner 1s electrons was found to be more important than that from the peak.

It has been found that the error due to the approximation never exceeds 0.2 % of the total scattering intensity for the scattering angles less than 35° and for the photon energy from 15 to 35 keV.

More important is the correction to the tabulated incoherent scattering factor S(K) for the experimental situation where the measurements were made in a constant-scattering angle mode as theoretically investigated by Bonham.[1)]

1) R.A. Bonham, Phys. Rev. A21, 2950(1981);erratum, ibid. A35,3964(1987).

Charge and Momentum Densities in Pressure-Induced Metallic InSb with NaCl Structure

T. KOBAYASI and H. HARA†

College of Medical Sciences, Tohoku University,
Seiryo, Sendai 980, Japan
†College of General Education, Tohoku University,
Kawauchi, Sendai 980, Japan

Pressure-induced InSb with rock-salt structure, obtained from amorphous phase at the pressure of ∿10 kbar, is experimentally confirmed to be metallic. Previously[1∿3], by performing a self-consistent total energy calculation, we discussed metallic stability of this material. In these papers, we found that the material is a system of a coexistence of the metallic and the strongly covalent properties. The momentum density distribution in the typically covalent semiconductors is rather insensitive to a bonding structure of electrons[4]. On the other hand, in metallic systems, it is indeed sensitive to an electronic structure. In view of these facts, it is interesting to study the charge and momentum densities of this material in detail.

In this paper, we calculate the Compton-profile and the positron annihilation angular correlation of this coexisting system. We discuss the extent of appearance of metallic characteristics in the covalent background. The results will also be discussed in connection with the charge distribution in real space, the charge transfer and the metallic stability.

[1] K.Shindo, S.Shimamura, T.Kobayasi and H.Hara: J.Phys.Soc.Jpn. 49 (1980) 2083.
[2] K.Shindo, T.Kobayasi and H.Hara: J.Phys.Soc.Jpn. 50 (1981) 2274.
[3] T.Kobayasi, K.Shindo and H.Hara: *Solid State Physics under Pressure*, ed. by S.Minomura (KTK Sci. Pub., Tokyo 1985), p49.
[4] H.Hara, K.Shindo and T.Kobayasi: J.Phys.Soc.Jpn. 46 (1979) 77. H.Hara, T.Kobayasi and K.Shindo: J.Phys.C: Solid State Phys. 17 (1984) 3967.

Investigation of Electronic Structure of Some Oxides by Compton Scattering Technique

Farid M. Mohammad, B.K. Sharma and B.L. Ahuja*

Department of Physics, University of Rajasthan, Jaipur-302004 Rajasthan, India

*Department of Physics, Jodhpur University, Jodhpur, India.

ABSTRACT

Compton scattering technique has been applied to investigate the electronic structure of V_2O_5, Nb_2O_5 and MoO_3. The measurements have been made using ^{241}Am Compton spectrometer. Theoretical Compton profiles were computed for various electron configurations for each case. Present measurements support complete transfer of valence electrons from metal to oxygen ions in agreement with recent photoemission results[1].

---

1. F. Werfel and E. Minni, J. Phys. C 16, 6091 (1983)

Electron Momentum Distribution in Zirconium and Cadmium

B.K. Sharma and B.L. Ahuja*

Department of Physics, University of Rajasthan, Jaipur-302004 (India)

*Present Address: Department of Physics, University of Jodhpur Jodhpur (Rajasthan), India

Abstract

Electron momentum distributions in hcp Zr and Cd have been studied for the first time using Compton scattering technique. Measurements have been made by scattering 59.54 keV gamma-rays. Theoretical computations have been carried out using Renormalised-Free-Atom model. Best agreement between theory and experiment is found if the electron configuration for Zr is chosen as $4d^3 5s^1$. For Cd, the RFA model predicts reasonably well the Compton profile in comparison to free electron and atomic models.

Compton Profile of Polycrystalline Tungsten

Usha Mittal, B.K. Sharma, Farid M. Mohammad and B.L. Ahuja*

Department of Physics, University of Rajasthan, Jaipur-302004, India

*Department of Physics, University of Jodhpur, Jodhpur (Rajasthan) India

ABSTRACT

Compton scattering technique has been applied to study the electron momentum distribution in polycrystalline tungsten. The measurements have been made using ^{241}Am γ-ray source (5Ci) and intrinsic Germanium detector. Experimental results have been compared with the band structure calculation of Papanicolaou et al[1] and with our Renormalised Free Atom Model (R.F.A.) calculations. R.F.A. values for $6s^1$ configuration are in better agreement with the experimental values.

1. N.I. Papanicolaou, N.C. Bacalis and D.A. Papaconstantopoulos Phys. Stat. Sol. (b) 137, 597 (1986).

THE CRYSTAL ELECTRON ENERGY AND COMPTON PROFILES FROM X-RAY DIFFRACTION DATA

ALEXANDROV JU. V., TSIRELSON V.G., OZEROV R.P.

Mendeleev Institute of Chemical Technology,
Miusskaja Sq. 9, 125820 Moscov, U.S.S.R.

There are several different quantum mechanic approaches to one-electron density matrix determination from X-ray diffraction data. The more general method of that kind which takes into account the crystal translation symmetry has been developed and is presented here. The method has been applied to electron energy and directed Compton profiles calculations of some covalent crystals-diamond and silicon. Kinetic energy (per atom in crystal) calculated practically coincides with the theoretical one and experimental values. The binding energies, which are determined as a difference of two very large values, coincides in 36%-limit; this limit is characteristic for Hartree-Fock calculation. Coincidence with theoretical data is better.

The directed Compton profiles had been calculated in momentum approximation. Good agreement with theory and experiment for both compounds in all regions studied has been obtained. We would like to draw attention that in the approach suggested the incoherent effects could be described starting with the coherent X-ray data. The fundamental role of the electron density can be seen here.

Directional Compton Profiles and their Fourier Transforms in GaAs

B.K. Panda, D.P. Mahapatra and H.C. Padhi

Compton profiles along the (100) and (111) directions of GaAs were measured using 59.54 kev gamma-rays from a 3 Ci annular source and an HPGe detector.

Compton profile as well as Fourier transformed Compton profile anisotropies are compared with pseudopotential calculations using both local [1] as well as local plus non-local [2] potentials. The measured Compton profile anisotropy (Fig.1) is found to be in reasonable agreement with theory for both sets of potentials. It can also be seen from Fig.1 that the extremums in the measured anisotropy are shifted slightly to higher q values as compared to theory. The autocorrelation anisotropy $\Delta B(111-100)$ as shown in Fig.2 is dominated by the bond anisotropy as in elemental semiconductors [3] and because of resolution the effects of second neighbour interaction cannot be seen. The negative peak in the anisotropy occurs at a position lower than the bond length (4.62 a.u). Some anisotropy is also found at about 1 a.u. which is not predicted by the theory. This suggests that the pseudopotential wavefunctions are not satisfactory close to the atomic centre which perhaps is evident from the fact that the wave-functions are not made orthogonal to the core electrons.

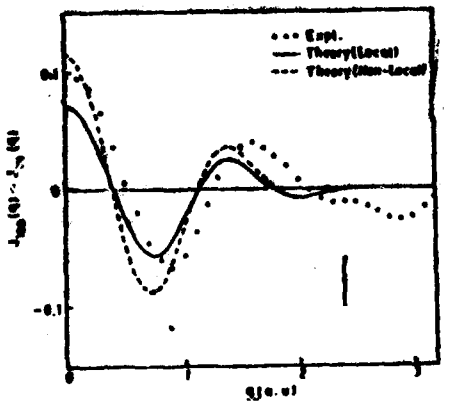

Fig.1

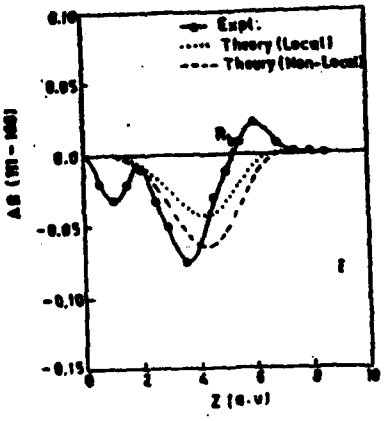

Fig.2

References:

1. M.L.Cohen and T.K.Bergstresser Phys. Rev.B 141 789 (1966).
2. J.R.Chetikowsky and M.L.Cohen, Phys. Rev. B 14 556 (1976).
3. P.Pattisin, N.K.Hansen and J.R.Schneider Chemical Physics 59 231 (1981).

P4 - Miscelaneous

Basis-Set Refinement by Cross - Entropy Minimization

Shridhar R. Gadre, Indira H. Shrivastava and Sudhir A. Kulkarni

Abstract

A general technique to refine a given atomic basis with the constraints of experimental / theoretical $\langle r^2 \rangle$ and $\langle p^2 \rangle$ values is presented. The refinement is achieved by minimization of the cross - entropy $S [\rho | \rho_0] = \int \rho(\vec{r}) \ln [\rho(\vec{r}) / \rho_0(\vec{r})] d\vec{r}$ where $\rho(\vec{r})$ and $\rho_0(\vec{r})$ are respectively the refined and reference (starting) densities. The wavefunctions are chosen to be Slater determinants. The procedure is tested on some Gaussian basis-sets for H, He, Li and Be atoms. It is found that the refined basis-sets yield, in general, excellent estimates of the $\langle r^n \rangle$ and $\langle p^n \rangle$ expectation values with relatively small loss in the total energy. Exploratory studies for molecules employing these refined sets are also presented.

---

* Abstract of the work to be presented at a Poster Session at SAGAMORE - IX to be held in Portugal in June - July, 1988.

P. Genoud, A. K. Singh, A. A. Manuel, T. Jarlborg, E. Walker, M. Peter

Département de physique de la matière condensée
Université de Genève
24, Quai Ernest Ansermet, CH-1211 Genève 4, Switzerland

and M. Weller

Max-Planck-Institut für Metallforschung
Institut für Werkstoffwissenschaften
Seestrasse 92, D-7000 Stuttgart, Germany

Electron momentum distribution and spin density of ferromagnetic iron studied by spin polarized positron annihilation

Abstract.
We report the first study of the Fermi surface topology, electron momentum density and spin momentum density in ferromagnetic iron using two-dimensional angular correlation of polarized positron annihilation radiation (2D-ACPAR). We have performed a self-consistent together with a parametrized band structure calculations using the linear muffin tin orbital (LMTO) method. Calculations of the momentum distributions were done both in the independent particle model approximation and including electron-positron correlation effects. The analysis of the experimental data shows that the large H-centered hole-ellipsoid of minority 3rd band given by the self-consistent band structure calculations does not exist or is very small. The nature of the electron-positron correlation effects is found to resemble the ones which were observed by Singh et al (*1986) for nickel. This confirms the systematic trends of the electron-positron correlation effects for localized d-electrons. The relative spin momentum density is negative at small values of p and can be correctly described only with a different treatment of the correlations for majority and minority electron bands.

*) A. K. Singh, A. A. Manuel, T. Jarlborg, Y. Mathys, E. Walker, M. Peter, 1986 Helv. Phys. Acta, 59 410

RESONANT RAMAN SCATTERING IN METALS

V. Eteläniemi, K. Hämäläinen, S. Manninen and P. Suortti

Department of Physics, University of Helsinki,
Siltavuorenpenger 20 D, 00170 Helsinki, Finland

S.P. Collins, M.J. Cooper and P.P. Kane

Department of Physics, University of Warwick,
Coventry, CV4 7AL, U.K.

In the resonant Raman scattering process (RRS) the incident x-ray photon energy is just below the the absorption threshold of the target electron. The intermediate state involves a virtual hole and in the final state there is a higher shell hole, an electron in the continuum and an emitted photon. The scattered energy spectrum is continuous because the photon and the ejected electron share the available energy. RRS arises from $\vec{p} \cdot \vec{A}$ term in the interacting Hamiltonian which couples the electromagnetic field and electron and the scattering cross section in dipole approximation has been recently calculated[1].

In order to study the energy dependence of the RRS cross section a tunable x-ray source is required. This can now be done using synchrotron radiation. Scattering components due to the A^2-term can be elimated by choosing a scattering angle of 90° and linearly polarised incident beam. First experiments of this kind were made for Ni in LURE, Paris[2].

In this study synchrotron radiation from SRS storage ring in Daresbury, U.K., was used to measure RRS cross section for Cu and Zn (K-shell hole) and Ho (L-shell hole). Incident x-ray energies varied from values ~ 1 keV below the absortion edge up to the energies ~ 300 eV above the edge where fluorescence was excited. The fluorescence yield was used to determine the incident photon flux and absolute RRS cross sections can then be obtained.

The double differential cross section $d^2\sigma/d^2\Omega d\omega$ of RRS in Ni was also measured using a high resolution crystal spectrometer and conventional x-ray tube[3]. This is particularly interesting because the cross section is modulated by the electron scattering from the neighbouring atoms. Similar effects are seen in EXAFS (Extended X-ray Absorption Fine Structure) but the role of the inner-shell hole is different.

[1] T. Åberg and J. Tulkki in "Atomic Inner-Shell Physics" edited by B. Crasemann (Plenum, New York, 1985) Ch. 10.
[2] S. Manninen, P. Suortti, M.J. Cooper, J. Chomilier and G. Loupias, Phys. Rev. B34, 353 (1986).
[3] P. Suortti, V. Eteläniemi, K. Hämäläinen and S. Manninen, J. Physique, to be published.

Binding and Correlation Effects in Simple Molecules As Studied by Gas-Phase X-Ray Diffraction

Keiko Nishikawa and Takao Iijima
Department of Chemistry, Gakushuin University
Toshima-ku, Tokyo 171, Japan

We reported gas-phase X-ray diffraction experiments carried out by the energy-dispersive method in order to investigate the binding and correlation effects in charge distribution of simple gaseous molecules. Comparison of the measured total (coherent + incoherent) intensities with the Hartree-Fock independent-atom calculation revealed the binding and correlation effects.[1)]

Recently improvement has been made in both the experiment and analysis. Reform of the gas cell has decreased the background intensity mainly caused by the scattering from the windows of the cell to 1/10.

For the inelastic cross section to be compared with experiment, a more rigorous expression for constant-angle measurements given by Bonham[2)] has been used instead of the Waller-Hartree theory.

When several angle-settings were made for covering a wide range of s-values (s: scattering parameter), the applied tube current was different for different scattering angles. This difference of the tube current might change the energy-spectrum of the white X-rays. This effect is now under investigation. The improved results of O_2 and Ne will be presented.

1) K. Nishikawa and T. Iijima, J. Chem. Phys., 87, 3753(1987).
2) R.A. Bonham, Phys. Rev., A23, 2950(1981); erratum, ibid., A35, 3964(1987).

HIGH ENERGY NEUTRON RECOIL SCATTERING IN LIQUID ^{4}He

R S Holt, L M Needham and M P Paoli

Neutron Division
Rutherford Appleton Laboratory
Chilton, Didcot, Oxon. U.K.

Abstract

Neutron recoil scattering from liquid ^{4}He at 4.2 K and 1.6 K has been observed for a momentum transfer of 150 $Å^{-1}$ using the electron volt spectrometer on the pulsed neutron source ISIS at the Rutherford Appleton Laboratory. The spectrometer is based on the (n,γ) neutron resonance absorption technique using a single Bismuth Germanate photon detector. Analysis of the recoil scattering spectra yielded mean atomic kinetic energy values $\langle K \rangle = 14.8 \pm 3.0$ K at 4.2 K and $\langle K \rangle = 14.6 \pm 3.2$ K at 1.6 K in good agreement with values obtained at much lower momentum transfer. No direct evidence for the Bose Condensate peak was found but an upper limit to the condensate fraction, n_o, of 20% was determined using model calculations. This value is in reasonable agreement with other condensate fractions reported in the literature at this particular temperature.

ANISOTROPY IN THE ATOMIC MOMENTUM DISTRIBUTION OF PYROLYTIC GRAPHITE

M P Paoli and R S Holt

Neutron Division
Rutherford Appleton Laboratory
Chilton, Didcot, Oxon. U.K.

Abstract

Deep inelastic neutron scattering using the (n,γ) resonance absorption technique on the pulsed source ISIS has been used to determine the mean atomic kinetic energy in pyrolytic and polycrystalline graphite. An analysis of the recoil distribution widths shows a significant anisotropy in the atomic momentum distribution measured parallel and perpendicular to the hexagonal layers. Comparison between the observed mean kinetic energies and those derived from a phonon density of states model are in agreement perpendicular to the layers but at variance parallel to the layers. A small asymmetry in the recoil line shape has also been observed and is attributed to the influence of final state corrections to the Impulse Approximation.

DETERMINATION OF ATOMIC MOMENTUM DENSITIES BY DEEP INELASTIC NEUTRON SCATTERING

R S Holt and M P Paoli

Neutron Division
Rutherford Appleton Laboratory
Chilton, Didcot, Oxon. U.K.

Abstract

The techniques of neutron resonance absorption have been used on the pulsed source ISIS at the Rutherford Appleton Laboratory to determine the atomic momentum distribution n(p) of light atoms. The high flux of epithermal neutrons allows strong neutron resonances in the electron volt region to be used. An (n,γ) or Resonance Detector Spectrometer (RDS) based on neutron TOF has been developed on ISIS using both single and multidetector configurations. The high energy gamma rays emitted after absorption are captured by Bismuth Germanate (BGO) photon detectors. The high momentum and energy transfers achieved using the RDS technique are necessary to validate the Impulse Approximation in the recoil scattering process allowing n(p) to be extracted from the measured S(Q,ε) spectra directly. Neutron recoil spectra (analogous to Compton profiles using photon scattering) therefore provides a direct method of determining atomic kinetic energies and atomic potentials. Recent measurements in polycrystalline Be are used to illustrate some of the aspects of this technique.

ELECTRIC FIELD GRADIENTS MEASURED ON THE SYSTEMS Nb-H AND Ta-H BY PERTURBED ANGULAR CORRELATIONS

J.M. Gil, P.J. Mendes, L.P. Ferreira, A.P. de Lima and N. Ayres de Campos

Physics Department, University of Coimbra, 3000 Coimbra, Portugal

Hydrogen atoms form interstitial sublattices when introduced in bcc Nb and Ta lattices, where they occupy tetrahedral sites [1]. Its structure is dependent on the hydrogen concentration and sample temperature. The phase-diagrams of these systems are known to a great extent, and some of the structures were determined by X-rays, neutron and TEM diffraction methods [1].

The Perturbed Angular Correlation techniques were applied successfully to those systems using ^{181}Hf radioactive atoms as substitutional probes in the metal lattice [2,3]. The technique yields information concerning the close vicinity of the probes, in the form of the electric field gradient (efg) measured at the probe nuclei.

Although the identification of some known phases could be done by unique efg sets, the interpretation of the efg themselves is not straightforward. Point charge models have been developed in the past to explain the efg values obtained in many different PAC experiments [4].

In the present work, the point charge model which usually only takes into account the positive charge of the ions of the lattice was improved by adding negative charges simulating the first moment of the electronic charge density around the probe atoms. The choice of the point charges and their localization was based on theoretical calculations of the changes induced on the electronic charge density by the introduction of a hydrogen atom in the metal lattice [5].

[1]-T. Schober, H. Wenzl, in "Hydrogen in Metals II", Top. in Appl. Phys., vol. 29, G. Alefeld, J. Voelkl (eds.), Springer, Berlin, 1978, p. 11.
[2]-P.J. Mendes, J.M. Gil, N. Ayres de Campos, R. Peichl, A. Weidinger, Hyp. Int., 15/16 (1983) 791.
[3]-J.M. Gil, P.J. Mendes, A.P. de Lima, N. Ayres de Campos, Sheng Yuqin, R. Peichl, A. Weidinger, J. of the Less-Common Met., 129 (1987) 145.
[4]-E. Dodenstedt, Hyp. Int., 24/26 (1985) 521.
[5]-H.C. Fritsche, F. Duebler, H. Mueller, Z. Anorg. Allg. Chem., 513 (1984) 46.

HYPERFINE INTERACTIONS AND ELECTRONIC STRUCTURE OF THE $FeNH_3$ MOLECULE

Joyce Terra and Diana Guenzburger
Centro Brasileiro de Pesquisas Físicas, Rio de Janeiro, Brasil

Fe atoms, when trapped in frozen NH_3 matrixes, react to form the molecules $FeNH_3$. This species provides a model for the study of the interaction of NH_3 with Fe surfaces. The Mössbauer spectrum shows two narrow peaks of equal intensity, which suggests a quadrupole interaction and a well-defined Fe site. The Isomer Shift measured is different from that of Fe atoms in rare gas matrixes. Mössbauer experiments in the presence of an external magnetic field reveal a large positive magentic hyperfine field (M. Saitovitch, Joyce Terra and M. Litterst, unpublished).

We have performed self-consistent all-electron Molecular Orbitals calculations for the $FeNH_3$ species which, combined with the experimental data, provide insight on the electronic structure of this molecule. The Discrete Variational method with the local density approximation was employed. The probable ground-state configuration is $\ldots a_1^1(\uparrow)e^2(\uparrow)e^2(\downarrow)a_1^0(\downarrow)$, and a Mulliken-type population analysis gives the Fe configuration $3d_\uparrow^5 3d_\downarrow^2 4s_\uparrow^{0.7} 4s_\downarrow^{0.3} 4p_\uparrow^{0.09} 4p_\downarrow^{0.02}$. The large positive calculated contact hyperfine field (+980 kG), obtained from the spin density at the Fe nucleus, in good accord with experiment, is mainly due to the large population of the Fe $4s_\uparrow$ orbital,

relative to $4s_{\downarrow}$. The Quadrupole Splitting calculated (-1.61 mm/s) also compares well with the experimental value. The calculated value of the charge density at the Fe nucleus is in good accord with the measured Isomer Shift. A small negative charge on Fe ($\sim$-0.1) is found, as expected from consideration of the N lone-pair donation to Fe.

ELECTRONIC STRUCTURE AND ISOMER SHIFTS OF Sn HALIDES

Joyce Terra and Diana Guenzburger
Centro Brasileiro de Pesquisas Físicas, Rio de Janeiro, Brasil

Measurements of the Isomer Shift δ of compounds by Mössbauer spectroscopy, combined with first-principles calculations of the electronic density at the nucleus of the probe atom $\rho(o)$, provide valuable information on the chemical bonding of the Mössbauer atom to its neighbors, besides making it possible to determine the nuclear parameter $\Delta R/R$, which is the relative change of the nucleus radius in the Mössbauer transition. We have made calculations of $\rho(o)$ for Sn halides (SnX_4, X = F, Cl, Br and I), using the all-electron self-consistent Discrete Variational method in the local density approximation. An embedding scheme was used to simulate the crystal. A very good linear relationship between $\rho(o)$ and δ was found, and the value $\Delta R/R = 2.2 \times 10^{-4}$ was derived. The increase in $\rho(o)$ from F to I is due mainly to the increase in the population of the 5s orbital of Sn.

LOCALIZATION OF ATOMIC IMPURITIES IN MINERALS BY PRECISION X-RAY DIFFRACTION DATA

V.S. URUSOV, E.L. BELOKONEVA

Moscow State University, Geological Faculty, Moscow

The improvement of X-ray diffraction experiment and treatment of the data has permited to make precision study of the crystal structure details and peculiarities of electron density distribution, i.e. chemical bond features. The first paper, which demonstrated the principal possibility of localization a small impurity amount in a structure by careful analyses of $\delta\rho$-maps, had dealt with ruby structure investigation [1]. It was detected the structure position of a small amount of Cr^{3+} (0,5wt%). Using such approach we studied three spinels: 1) noble $MgAl_2O_4$ (0,8wt%Fe) [2], 2) hercynite [3], 3) syntetic Co-spinel? and five berylls: 4) practicaly pure beryll [4], 5) aquamarine (2,4wt%Fe), 6) smaragd (0,3wt%Cr, 0,3Fe, 2,0%g), syntetic 7) Co- (1,1wt%) and 8) Cu- (1,8wt%) -bearing berylls. The experimental data were obtained by "Syntex" P1, the structures were refined using an "Eclipse-S/200" computer by INEXTL-programs. The reliability factors R, R_w and goodness of fit S for high-order region of reciprocal space are in the table. The atructure positions of small amount of impurities are important for physical properties interpretation, especially magnetic and spectral ones. The $\delta\rho$-maps allowed to detect chemical bond peculiarities in spinels as well as in ring-silicate beryll.

Table.

	sample							
	1)	2)	3)	4)	5)	6)	7)	8)
R,%	0,77	0,88	1,07	0,73	1,17	1,31	1,08	1,44
R_w,%	0,96	1,35	1,52	0,79	1,40	1,49	1,02	2,33
S	1,008	1,358	0,881	1,020	0,933	1,010	1,076	1,596

*The experimental data were kindly sent by Prof. Y. Saito

1. V.G. Tsirelson, M.Yu. Antipin, R.G. Gerr, R.P. Ozerov, Yu. T. Struchkov, Phys. Stat. Sol. (a) 87, 425, 1985. 2.V.G. Tsirelson, E.L. Belokoneva, Yu. Z. Nozik, V.S. Urusov, Geochimija, N7, 1033, 1986. 3. V.A. Streltzov, E.L. Belokoneva, V.G. Tsirelson, V.S. Urusov, R.P. Ozerov, Geochimija, N10, 1456, 1987. 4. O.A. Evdokimova, E.L. Belokoneva, V.G. Tsirelson, V.S. Urusov, N5, 1988.

THE X-RAY PSEUDOPOTENTIAL FOR A^{IV}, $A^{II}B^{VI}$ AND $A^{III}B^{V}$ COMPOUNDS, DETERMINED USING THE COHERENT AND NONCOHERENT SCATTERING FACTORS By J.Jakimavichius, Vilnius Institute of Building Engineering, Vilnius, USSR

The X-Ray pseudopotential components (XPC) for A^{IV},$A^{II}B^{VI}$ and $A^{III}B^{V}$ compounds related with the charge density distribution in the crystals have been obtained using the measured structure amplitudes and noncoherent scattering factors. The OPW approximation for valence electron wave functions and first order of overlap integrals have been used. These approximations, as it was shown in (J.Jakimavichius, J.Batarūnas, Molecule Physics, Kiev, 1976, N 2, p.61) lead to the XPC matrix elements $V_k(\vec{S})=\frac{4\pi}{v_0 S^2}\left[f_v(\vec{S})-\sum_i f_{ti}(\vec{S}-\vec{k})f_{ti}(\vec{k})-\sum_i f_{ti}(\vec{S}-\vec{k})f_{ti}(\vec{k})\right]$, expressed in terms of coherent $f_v(\vec{S})$ and noncoherent (Compton) $f_{ti}(\vec{S}-\vec{k})=\int|\varphi_{ti}|^2\exp i(\vec{S}\vec{r})\,d\vec{r}$ scattering factors. The valence electron scattering amplitudes or factors have been separated from the measured values $f_{exp}(\vec{S})$ according to $f_v(\vec{S})=f_{exp}(\vec{S})-f_c(\vec{S})$, where $f_c(\vec{S})$ - is the core scattering factor.

The XPC and energy levels in the points Γ, X, L and along lines Δ and Λ for the Si, ZnS, ZnSe, ZnO, CdS, CdSe, CdTe, BN and GaAs compounds has been investigated. The values of XPC and energy levels for ZnSe as the illustration of the method are presented in the table

HKL	$V_{exp}(S)$	V_{XPC}	$V(S)_o$	Method Osp	ΔE_{XPC} (eV)	Optical E_{XO} results (eV)
III	2,49	2,76	2,72	$\Gamma_{1c}-\Gamma_{15v}$	3,0	2,9
200	-1,54	-1,63	-1,87	$\Gamma_{15c}-\Gamma_{15v}$	7,8	-
220	-0,07	0,14	0,16	$L_{1c}-L_{3v}$	4,7	4,9
311	-0,06	0,63	0,13	$X_{1c}-X_{5v}$	6,1	6,4

Here $V(S)_{exp}$-potential components, determined by use of the experimental structure amplitudes, $V(S)_{XPC}$-determined with taking into account the nonlocal part of pseudopotential, $V(S)_{op}$-optical pseudopotential components. The main parts of XPC are expressed by the local part determined using the experimental values of $P(S)_{exp}$. The energy levels in the basis of V_{XPC} and superposition of simmetrical plane vawes have been determined. The agreement of energy gaps calculated using the measured scattering amplitudes with optical experimental results has been observed. The dependance of energy levels and XPC on pecularities of charge density distribution and effective charge of ions in the investigated compounds has been discussed.

THE VALENCE ELECTRON MOMENTUM DISTRIBUTION INVESTIGATION IN THE SUPERIONIC β - AND β'' - $Na_2O \cdot x\, Al_2O$ COMPOUNDS

By J.Jakimavichus, Vilnius Institute of Building Engineering., A.Alishauskas and R.Purlys, Faculty of Physics, Vilnius University, Vilnius, USSR

The valence electron momentum distribution functions (VEMDF) of superionic compounds β - and β'' - $Na_2O \cdot x\, Al_2O_3$ have been investigated by use of the measured and calculated Compton profiles (CP). The dependence of CP and VEMDF on the change of lattice structure of hexagonal β - and β'' - aluminates has been investigated. The influence of stoichiometric composition of - aluminates to the CP and VEMDF has been studied. The X-Ray three--crystal spectrometer for Compton lines measurements has been used. The scattering angle was 120^0. The monochromatic Mo K_{α_1} ($h\nu$ = 17, keV) radiation has been used. The monochromatization of Mo X-Ray radiation was performed by Ceylon graphite. The Li served as crystal - analyser. The exposure time was 200 s per point. The noncoherent scattering factors, calculated with taking into account the ionization of atoms for normalization of measured Compton lines have been used. The calculated CP and VEMDF with taking into account the ionization of atoms Na^+, Al^{3+}, O^{2-} for comparision with the experimentally obtained results have been applied.

The decrease of measured CP as compared with the calculated ones, including superposition of free atoms in the low momentum region for β - and β - aluminates has been observed. This decrease of measured CP corresponds to the shift of VEMDF to the region of higher momentum. Taking into consideration the ionization of atoms Al^{3+}, N^{1+}, O^{2-} leads to better agreement between measured and calculated CP. The correlation of valence electron distribution in real and impulse space has been investigated. The increase in charge density in the region of wave function maximum and displacement to the nuclei in real space have been observed. The influence of electron structure change, caused by ionization of atoms and charge density deformation to CP and VEMDF have been discussed.

Author Index